Available online at www.sciencedirect.com
ScienceDirect
Journal of Molecular Graphics and Modelling 26 (2008) 982–990
Journal of Molecular Graphics and Modelling
www.elsevier.com/locate/JMGM

Conformational analysis of alkali metal complexes of anionic species of aspartic acid, their interconversion and deprotonation: A DFT investigation

Wichien Sang-Aroon, Vithaya Ruangpornvisuti *

Supramolecular Chemistry Research Unit, Department of Chemistry, Faculty of Science, Chulalongkorn University, Bangkok 10330, Thailand

Received 20 June 2007; received in revised form 10 August 2007; accepted 14 August 2007
Available online 19 August 2007

Abstract

Gas-phase geometry-optimized structures of aspartate complexes of anionic species ($Hasp^-$) with lithium, sodium and potassium metal cations and transition-state structures for their interconversions were obtained using the density functional theory computations at the B3LYP/6-311++G(d,p) level of theory. The metal ion affinities of $Hasp^-$ species and deprotonation energies of [Hasp-M] complexes, M = Li^+, Na^+ and K^+, and their conformers were obtained. Relative energies of the [Hasp-M] complex conformers, reaction energies, thermodynamic properties, rate and equilibrium constants of their complexation are reported. Binding energies of the most stable complexes with Li^+, Na^+ and K^+ are −168.53, −133.34 and −117.68 kcal/mol, respectively. The most stable complex conformer as a tri-coordinated form for aspartate complex with Li^+ and bi-coordinated form for aspartate complexes with Na^+ and K^+ were found.

Keywords: Complexation; Aspartate anion; Alkali cation; Lithium; Sodium; Potassium; Metal ion affinity

1. Introduction

Alkali metal ions; lithium, sodium and potassium have been found in biological systems. They play a crucial role in many biological processes by interacting with a variety of peptides or proteins [1]. The cations interact with proteins and peptides to control structural and regulating properties [2–5], transport process through transmembrane channels [6,7]. The location of different metal ions in the hydrophobic cavity of a protein depends preferentially on the relative intrinsic bond strength between the metal ions and the various possible metal binding sites. The chemistry of cationized-amino acids or oligopeptides systems has been wildly investigated by both experimental and theoretical approaches to gain better understanding their preferred binding locations and affinities. The gas-phase structures of cationized arginine with alkali metal ions were studied both by density functional theory calculations and experimentally using low-energy collisionally activated and thermal radiative dissociation [8] and glycine complexes with and divalent alkaline earth metal ions were studied by Hartree–Fock method [9]. Complexes of glycine, alanine and praline with alkali metal ions have been studied by DFT method [10–12]. Gas-phase intramolecular proton transfer in various metal cation complexes with glycine and chlorine substituted derivatives have been studied [13]. Non-zwitterionic and zwitterionic forms of glycine and their complexes with alkali, alkaline earth and transition metal ions hydrated with two and five water molecules were studied by DFT methods [14]. The salt bridging is one of the non-covalent interaction as well as hydrogen bonding, hydrophobic effect and cation–π interaction. These interactions regulate the biological functions of proteins or enzymes. For example, salt bridging is play an important role in assembly of some protein multimers [15], enzyme-receptor recognition [16], peptide fragmentation [17–19] where as the cation–π interaction are believed to be responsible for the ion selectivity of potassium channels [20,21]. Ion mobility [22,23], black body infrared radiative dissociation (BIRD) [24–29], kinetic method [30,31], H/D exchange [32,33] and guide ion beam mass spectrometry [34–37] have been widely used to determine the cationized-amino adducts.

* Corresponding author. Tel.: +66 2218 7644; fax: +66 2254 1309.
E-mail address: vithaya.r@chula.ac.th (V. Ruangpornvisuti).

1093-3263/$ – see front matter
doi:10.1016/j.jmgm.2007.08.004

However, many previous works have been determined the cationized adducts of neutral and zwitterionic forms of amino acid to compare the preference between charge solvated (CS) and salt-bridge (SB) structure [8–13,15]. In fact, amino acids possess not only the zwitterionic form but also cationic and anionic forms in a wide pH range of acidic to basic aqueous solution. Aspartic acid as well, the conformational equilibria of cationic (H_3asp^+), zwitterionic (H_2asp), anionic ($Hasp^-$) and dianionic (asp^{2-}) species were presented within a wide pH range. The conformational structures of various ionic species of gas-phase aspartic acid have been theoretically determined [38]. Experimentally, the lithium and sodium affinities of zero net charge aspartic acid have been determined by Feng et al [39] and Kish et al. [40], respectively. In previous work, the cationized-complexes of aspartate dianion (asp^{2-}) with Li^+, Na^+ and K^+ and their interactions in gas phase were theoretically determined [41]. There are still no works studied on anionic ($Hasp^-$) complexes with alkali metal cations in the literature survey. Thus, the present work is to elucidate the binding modes of interactions between alkali cations; Li^+, Na^+ and K^+ and zwitteranionic species of aspartic acid by means of theoretical approach. The conformational preferences as well as metal ion affinities (MIA) of the complexes will be determined. Because $Hasp^-$ species can deprotonate their acidic proton, so the deprotonation energy (DPE) of the cationic complexes is also determined. Based on the gas-phase conformations of $Hasp^-$, the conformational changes between free and complex forms of the aspartate ligand will be presented.

2. Computational details

The geometry optimizations of [Hasp-M], M = Li^+, Na^+ and K^+ complexes structures were carried out using density function theory (DFT). The DFT computations have been performed with Becke's three parameters hybrid density functional using the Lee, Yang and Parr correlation functional (B3LYP) [42,43]. The B3LYP/6-311++G(d,p) level of theory has been employed for all geometry optimizations and their thermodynamic properties were derived from the vibrational frequency computations at the same level. The solvation effects were taken into account by single-point computations on the B3LYP/6-311++G(d,p)-optimized gas-phase structures using in conductor-like polarizable continuum model (CPCM) [44]. Counterpoise corrections were applied for energy improvement by eliminating the basis set superposition error (BSSE) [45,46] for the most stable complex conformers. All computations were performed with the GAUSSIAN 03 program [47]. The MOLDEN 4.2 program [48] was utilized to display molecular structures, monitor the geometry convergence via the Gaussian output files. The molecular graphics of all complexes were generated with the MOLEKEL 4.3 program [49].

As metal ion affinity (MIA) is defined as the negative of the reaction enthalpy (ΔH°), the MIA for the complexation of [Hasp-M] described by reaction $Hasp^- + M^+ \rightarrow$ [Hasp-M] was computed using the following equation:

$$\mathrm{MIA} = -[H^\circ_{[\mathrm{Hasp-M}]} - (H^\circ_{[\mathrm{Hasp}^-]} + H^\circ_{[\mathrm{M}^+]})] \quad (2.1)$$

where the [Hasp-M] complex is formed from the $Hasp^-$ species and M^+ alkali metal cation. The standard enthalpy ΔH°_{298} and Gibbs free energy changes ΔG°_{298} of complexation reactions were obtained by the thermodynamical analysis at 298 K, 1 atmosphere using the vibrational frequency calculations at the B3LYP/6-311++G(d,p) level of theory. As deprotonation energy (DPE) is defined as the reaction energy described by

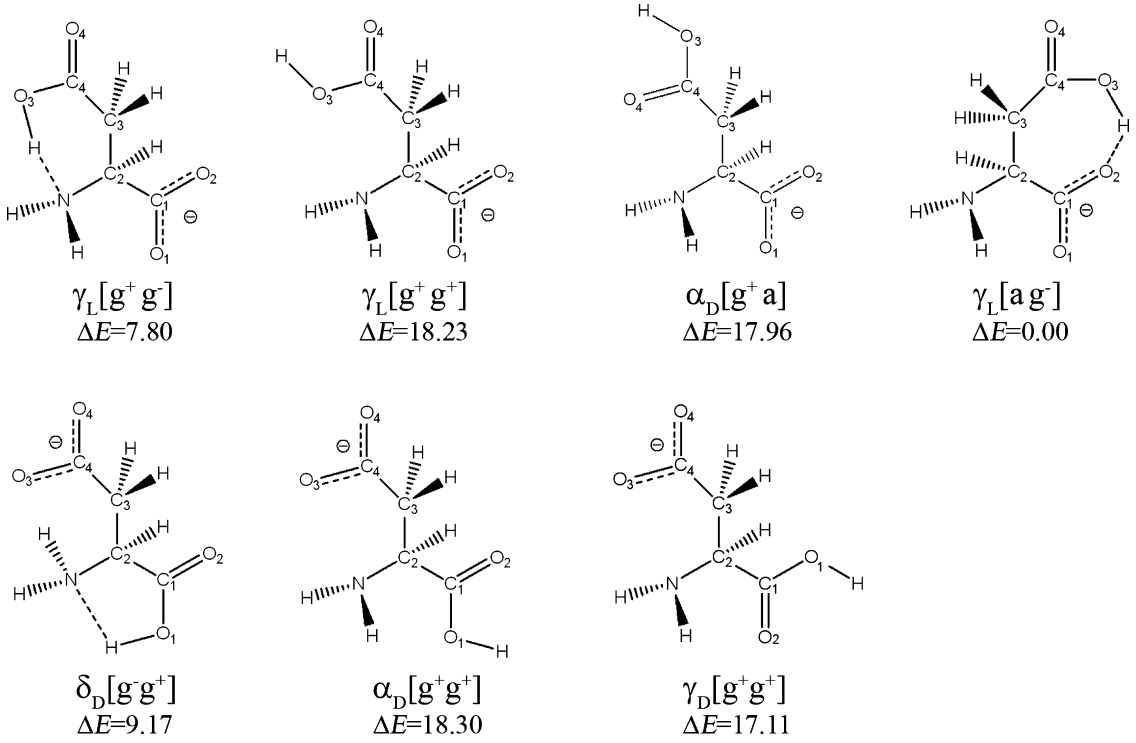

Fig. 1. The B3LYP/6-311++G(d,p)-optimized structures of $Hasp^-$ ligand.

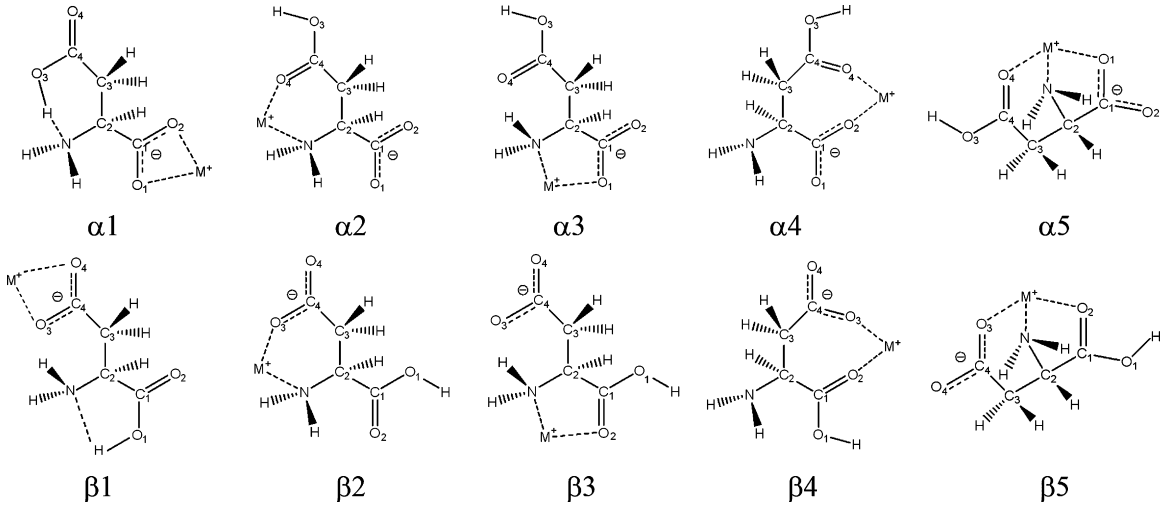

Fig. 2. The possible binding modes of $Hasp^-$ ligand toward cations.

[Hasp-M] → $[Asp-M]^- + H^+$, the DPE of the [Hasp-M] complex was obtained using the following formula:

$$DPE = (E^\circ_{[aspM^-]} - E^\circ_{[H^+]}) - E^\circ_{[Hasp-M]} \quad (2.2)$$

where the $E^\circ_{[aspM^-]}$, $E^\circ_{[H^+]}$ and $E^\circ_{[Hasp-M]}$ are energies of deprotonated species, free proton and [Hasp-M] complex species, respectively. The structures and energies of $[asp\_M]^-$ complexes corresponding to their [Hasp_M] complexes were taken from our previous work [40] calculated at the same level of theory.

3. Results and discussion

The B3LYP/6-311++G(d,p)-optimized structures of free-form zwitter-anionic conformers ($Hasp^-$) based on two conformational types of α-[NH_2·CH(CH_2·COOH)COO^-] and β-[NH_2·CH(CH_2·COO^-)COOH] are shown in Fig. 1. It shows that there are at least seven types of free-form conformers of [Hasp-M], M = Li^+, Na^+, K^+ complexes as four α-[Hasp-M] and three β-[Hasp-M] complexes species. Possible binding modes of $Hasp^-$ aspartate binding atoms toward the alkali metal cations, M = Li^+, Na^+, K^+ are defined as displayed in Fig. 2. As 10 possible binding modes, five for α-[Hasp-Li] and another five for β-[Hasp-Li] are defined as single binding mode, others combined modes can be possibly defined as combination of these single modes such as a combined mode of α1 + α2. As the binding mode is defined as the ratio of the number of metal ion (N_M) to the number of binding site of the ligand (N_L), the N_M:N_L ratios are 1:1 for binding mode types α1 and β1, 1:2 for types α2–α4 and β2–β4, and 1:3 for types α5 and β5.

3.1. Lithium aspartate complexes

The B3LYP/6-311++G(d,p)-optimized structures of α- and β-[Hasp-Li] complex conformers and their conversion reactions are shown in Figs. S1 and S2, Supplementary data, respectively. At least a transition state for interconversion between two [Hasp-Li] complex conformers has been found. All transition-state structures for lithium aspartate complex system are shown in Figs. S3 and S4, and their cartesian coordinates are given in Table S1. Eleven and seventeen interconversion equilibria for α- and β-[Hasp-Li] complexes conformers were found respectively and categorized as five single-step and three double-steps reactions for α-[Hasp-Li] complex system, and two single-step, two double-steps, one tetra-steps and one hepta-steps reactions for β-[Hasp-Li] complex system as shown in Figs. S1 and S2. The most stable conformer of [Hasp-Li] complex system is the conformer **19** as shown in Fig. 3. The gas and aqueous phase relative B3LYP/6-311++G(d,p) energies, MIAs and DPEs for [Hasp-Li] complex species are tabulated in Table 1. It shows that [Hasp-Li] complex conformers are mostly in the single binding mode, except conformers **7–11** for α-[Hasp-Li] complex type,

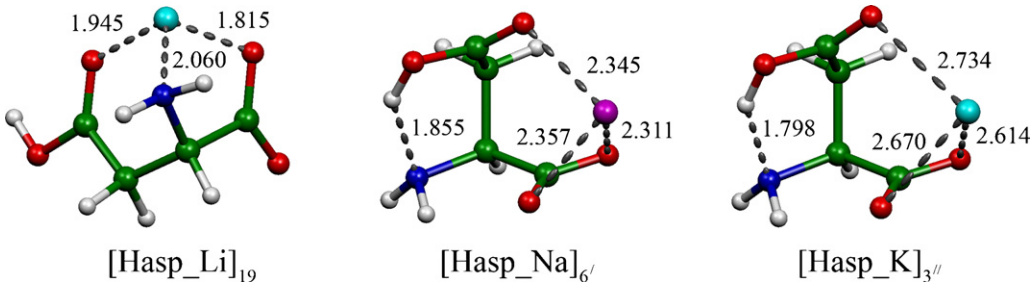

Fig. 3. The most stable conformer of [Hasp_Li], [Hasp_Na] and [Hasp_K] complexes in gas phase. Distances are in Å.

Table 1
Relative B3LYP/6-311++G(d,p) energies, MIAs and DPEs for α-[Hasp-Li] and β-[Hasp-Li] complexes

Complexes/ systems	Aspartate conformations	Binding mode	ΔE^a	MIA[a]	DPE[a]
α-[Hasp-Li]					
1	γ_L [g$^+$g$^-$][b]	α1	10.80	148.11	336.70
2	γ_L [g$^-$ g$^-$][c]	α1	7.30	161.92	340.20
3	γ_L [g$^-$ a][d]	α1	5.65	163.90	341.84
4	γ_D [a a][e]	α1	7.33	161.85	340.16
5	α_D [a g$^+$][f]	α1	8.27	161.17	339.23
6	α_D [a g$^-$][g]	α1	4.20	147.31	343.29
7	α_L [g$^+$g$^-$][h]	α1 + α4	9.18	150.49	316.17
8	γ_D [g$^+$ a][i]	α1 + α4	2.70	166.86	322.66
9	γ_D [g$^+$g$^+$][j]	α1 + α4	8.47	160.55	316.89
10	γ_D [a g$^-$][k]	α1 + α4	9.14	160.86	338.35
11	γ_D [a g$^+$][l]	α1 + α4	3.44	166.65	344.05
12	γ_L [g$^-$ g$^+$][m]	α2	31.72	138.08	302.59
13	γ_D [g$^-$ g$^-$][n]	α2	24.07	145.55	310.24
14	δ_D [g$^-$g$^+$][o]	α3	8.16	142.75	330.03
15	δ_D [g$^-$ a][p]	α3	7.24	162.41	330.95
16	γ_L [a g$^-$][q]	α4	13.52	156.36	308.16
17	γ_L [a g$^+$][r]	α4	6.44	163.24	315.24
18	δ_D [g$^+$ g$^-$][s]	α5	6.72	163.22	312.36
19	δ_D [g$^+$ a][t]	α5	0.00	169.76	319.09
β-[Hasp-Li]					
20	ε_D [g$^-$g$^+$][a1]	β1	7.46	154.65	339.71
21	γ_D [g$^-$ g$^+$][b1]	β1	8.24	155.06	338.94
22	δ_D [g$^-$g$^+$][c1]	β1	5.00	140.34	342.17
23	γ_D [a g$^-$][d1]	β1	9.22	153.96	337.95
24	ε_D [a a][e1]	β1	8.55	153.44	338.63
25	ε_D [a g$^-$][f1]	β1	5.30	149.03	341.88
26	γ_D [g$^-$g$^+$][g1]	β2	11.42	152.02	322.90
27	γ_D [g$^-$g$^+$][h1]	β2	9.24	153.03	327.16
28	ε_D [g$^-$g$^+$][i1]	β1 + β2	9.02	153.41	327.37
29	γ_D [g$^-$g$^+$][j1]	β1 + β2	10.83	152.79	336.35
30	δ_D [g$^-$g$^+$][k1]	β3	34.48	129.15	303.72
31	β_L [g$^-$g$^+$][l1]	β3	27.74	134.83	310.45
32	δ_D [g$^+$g$^+$][m1]	β5	7.43	156.31	311.66
33	β_L [g$^+$g$^+$][n1]	β5	3.09	159.46	315.99
34	β_L [a g$^+$][o1]	β4	19.12	142.92	302.56
35	δ_D [a g$^+$][p1]	β4	11.98	151.37	309.70
36	δ_D [a g$^-$][q1]	β4	5.04	149.44	316.64
37	β_L [a g$^-$][r1]	β1 + β4	12.53	149.60	311.61
38	δ_L [a g$^-$][s1]	β1 + β4	7.94	155.72	316.20
39	α_D [a g$^-$][t1]	β1 + β4	2.20	152.50	321.94

[a]In kcal/mol with ZPE correction. [b]Identical to δ_L [g$^-$ g$^+$]. [c]Identical to δ_L [g$^-$ g$^+$]. [d]Identical to δ_L [g$^-$ a]. [e]Identical to α_L [a a]. [f]Identical to γ_L [a g$^+$]. [g]Identical to γ_L [a g$^-$]. [h]Identical to δ_D [g$^+$ g$^-$]. [i]Identical to γ_D [g$^+$ a]. [j]Identical to γ_D [g$^+$ g$^+$]. [k]Identical to α_L [a g$^-$]. [l]Identical to δ_L [a g$^+$]. [m]Identical to γ_L [g$^-$ g$^+$]. [n]Identical to γ_L [g$^-$ g$^-$]. [o]Identical to α_L [g$^-$ g$^+$]. [p]Identical to δ_D [g$^-$ a]. [q]Identical to ε_L [a g$^-$]. [r]Identical to ε_L [a g$^+$]. [s]Identical to β_L [g$^+$ g$^-$]. [t]Identical to β_L [g$^+$ a]. [a1]Identical to γ_D [g$^-$ g$^+$]. [b1]Identical to ε_D [g$^-$ g$^+$]. [c1]Identical to β_L [g$^-$ g$^+$]. [d1]Identical to ε_D [a g$^-$]. [e1]Identical to γ_D [a a]. [f1]Identical to γ_D [a g$^-$]. [g1]Identical to δ_D [g$^-$ g$^+$]. [h1]Identical to β_L [g$^+$ g$^+$]. [i1]Identical to δ_D [g$^+$ g$^+$]. [j1]Identical to δ_D [a g$^+$]. [k1]Identical to β_L [a g$^+$]. [l1]Identical to β_L [a g$^-$]. [m1]Identical to δ_D [a g$^-$].

conformers **28**, **29**, **37–39** for β-[Hasp-Li] complex type. The relative stabilities are in decreasing order: **19**> **39**≈**8** > **33**≈**11**> **6**> **22**≈**36**≈**25**≈**3**> **17**> **18**> **15**≈**2**> **4**≈**32**≈**20** > **38** ≈ **14** ≈ **21** ≈ **5** ≈ **9** ≈ **24**> **28**>**10** ≈ **29** ≈ **7**≈ **27**> **1**> **26**> **35**> **37**> **16**≫ **34**> **13**> **31**> **12**> **30.**. Maximum values of MIA and DPE are found in the conformers **19** and **11**, respectively. The MIAs and DPEs of all [Hasp-Li] complexes are within 129.15–169.76 kcal/mol and 302.56–344.05 kcal/mol, respectively. Interconversion reactions between 2 of 39 [Hasp-Li] complexes with their transition states and their energies, thermodynamic properties, rate and equilibrium constants are shown in Table 2. Based on our previous work on dianionic-cation [asp_M]$^-$ complexes [41], the most stable complex conformer of [Hasp_Li] is similar to [asp_Li]$^-$. The Hasp$^-$ in the complex form adopted to be tri-dentate ligand binding with lithium cation by using N-amino, α- and β-oxygen atoms, respectively. The aspartic acid ligand in either [Hasp_Li] or [asp_Li]$^-$ complexes are similar in backbone conformation (δ_D) but slightly different in side-chain conformation (g$^+$a for [Hasp_Li] and g$^+$g$^+$ for [asp_Li]$^-$). MIA of [Hasp_Li] (169.76 kcal/mol) is very lower than that of [asp_Li] (254.86 kcal/mol).

3.2. Sodium aspartate complexes

The B3LYP/6-311++G(d,p)-optimized structures of [Hasp-Na] complex conformers and their conversion reactions are shown in Figs. S5 and S6. At least a transition state for interconversion between two [Hasp-Na] complex conformers has been found. All transition-state structures for sodium aspartate complex system are shown in Fig. S7 and their cartesian coordinates are given in Table S1. Seven and six interconversion equilibria for α- and β-[Hasp-Na] complexes conformers were found respectively and categorized as three single-step and two double-steps reactions for α-[Hasp-Na] complex system, and four single-step and one double-steps for β-[Hasp-Na] complex system as shown in Figs. S5 and S6. The most stable conformer of [Hasp-Na] complex system is the conformer **6′** as shown in Fig. 3. The gas and aqueous phase relative B3LYP/6-311++G(d,p) energies, MIAs and DPEs for [Hasp-Na] complex species are tabulated in Table 3. It shows that [Hasp-Na] complex conformers are mostly in the single binding mode, except conformers **4′**–**6′**, **9′** and **10′** for α-[Hasp-Na] complex type, conformers **18′**, **19′**, **22′** and **23′** for β-[Hasp-Na] complex type. The relative stabilities are in decreasing order: **6′**> **23′**> **5′**> **10′**> **3′**= **17′**> **12′**> **8′**> **15′**> **1′**> **22′**> **2′** = **21′**≈ **13′**> **7′**> **14′**> **16′**= **19′**> **9′**> **4′**> **18′**> **11′**> **20′.** Maximum values of MIA and DPE are both found in the conformer **5′**. The MIAs and DPEs of all [Hasp-Na] complexes are within 121.58–142.21 kcal/mol and 317.95–348.91 kcal/mol, respectively. Interconversion reactions between 2 of 23 [Hasp-Na] complexes with their transition states and their energies, thermodynamic properties, rate and equilibrium constants are shown in Table 4. Interestingly, the most stable complex conformer of [Hasp_Na] is different to its corresponding dianionic complex [asp_Na]$^-$. The aspartic ligand adopted as γ_D conformer either in [Hasp_Na] or [asp_Na]$^-$ but different in binding mode of interaction. For the anionic complex, the asp^{2-} ligand binds preferentially with sodium cation as tridentate binding mode using N-amino, α- and β-oxygen atoms, respectively. But for anionic complex [Hasp_Na], the Hasp$^-$ ligand preferred to bind with the cation using two α-oxygen and one β-oxygen atoms, respectively.

Table 2
Thermodynamic quantities, equilibrium and rate constants of conversion reactions of the [Hasp-Li] complex systems, computed at B3LYP/6-311++G(d,p) level of theory

Reactions/systems[a]	$\Delta^{\ddagger}E$[b]	$\Delta^{\ddagger}G$[b]	ΔE_{298}[b]	ΔH_{298}[b]	ΔG_{298}[b]	K_{298}	k_{298}[c]
1 → TSr1_2 → 2	31.15	31.30	−3.50	−3.26	−3.74	5.51×10^{2}	7.05×10^{-11}
2 → TSt2_3 → 3	10.06	11.00	−1.65	−1.70	−1.42	1.09×10^{1}	5.35×10^{4}
4 → TSt4_5 → 5	32.61	32.92	0.94	0.97	0.73	2.9×10^{-1}	4.56×10^{-12}
5 → TSr5_6 → 6	6.30	7.58	−4.07	−4.73	−1.52	$1.3.0 \times 10^{1}$	1.72×10^{7}
7 → TSr7_8 → 8	27.69	28.51	−5.77	−5.83	−4.76	3.09×10^{0}	7.19×10^{-9}
8 → TSt8_9 → 9	10.47	10.88	6.49	6.60	6.38	2.09×10^{0}	6.62×10^{4}
10 → TSt10_11 → 11	27.92	28.31	−6.72	−6.82	−6.19	3.43×10^{4}	1.09×10^{-8}
12 → TSt12_13 → 13	27.72	27.83	−5.70	−5.81	−5.64	1.34×10^{4}	2.47×10^{-8}
14 → TSt14v15 → 15	33.73	34.34	−0.92	−1.70	−0.18	1.34×10^{0}	4.14×10^{-13}
16 → TSt16_17 → 17	27.38	27.45	−7.65	−7.76	−7.56	3.50×10^{5}	4.66×10^{-8}
18 → TSt18_19 → 19	10.60	11.00	−1.65	−1.70	−1.42	1.09×10^{1}	5.35×10^{4}
20 → TSt20_21 → 21	32.98	32.98	0.77	0.80	0.71	3.06×10^{-1}	4.16×10^{-12}
21 → TSr21_22 → 22	10.62	10.80	−3.23	−3.60	−2.50	6.82×10^{1}	7.46×10^{4}
23 → TSt23_24 → 24	31.16	31.67	−0.68	−0.66	−0.62	2.86×10^{0}	3.76×10^{-11}
24 → TSr24_25 → 25	7.16	7.98	−3.25	−3.54	−2.24	4.39×10^{1}	8.77×10^{6}
26 → TSt26_27 → 27	32.27	32.39	−2.18	−2.20	−2.15	3.76×10^{1}	1.12×10^{-11}
27 → TSr27_29 → 29	2.61	3.70	−0.21	−0.38	0.65	3.30×10^{-1}	1.20×10^{10}
28 → TSt28_29 → 29	34.03	33.94	1.80	1.81	1.68	5.83×10^{-2}	8.21×10^{-13}
26 → TSr26_28 → 28	2.47	3.49	−0.59	−0.77	0.19	7.31×10^{-1}	1.72×10^{10}
30 → TSt30_31 → 31	28.97	29.25	−6.74	−6.87	−6.44	5.25×10^{4}	2.24×10^{-9}
32 → TSt32_33 → 33	30.73	30.87	−4.33	−4.35	−4.31	1.45×10^{3}	1.45×10^{-10}
34 → TSt34_35 → 35	26.74	26.72	−7.41	−7.26	−6.80	9.74×10^{4}	1.60×10^{-7}
35 → TSr35_36 → 36	8.82	9.31	−6.94	−7.19	−6.53	6.12×10^{4}	9.29×10^{5}
35 → TSr35_38 → 38	0.54	1.87	−4.04	−4.34	−2.71	9.64×10^{1}	2.63×10^{11}
34 → TSr34_37 → 37	0.0013	1.61	−6.59	−6.68	−5.64	1.35×10^{4}	4.09×10^{11}
37 → TSt37_38 → 38	32.86	32.88	4.59	4.93	3.88	1.44×10^{-3}	4.91×10^{-12}
38 → TSr38_39 → 39	12.85	12.02	−5.74	−5.91	−5.51	1.10×10^{4}	9.64×10^{3}
36 → TSr36_39 → 39	13.31	14.24	−2.83	−3.06	−1.69	1.73×10^{1}	2.26×10^{2}

[a] The letters 'r' and 't' specify for the rotational (about C_{β}–CO_2 bond) transition-state and proton-transfer transition-state, respectively.
[b] In kcal/mol.
[c] In s^{-1}.

3.3. Potassium aspartate complexes

The B3LYP/6-311++G(d,p)-optimized structures of [Hasp-K] complex conformers and their conversion reactions are shown in Figs. S8 and S9. At least a transition state for interconversion between two [Hasp-K] complex conformers has been found. All transition-state structures for potassium aspartate complex system are shown in Fig. S10 and their Cartesian coordinates are given in Table S1. Six interconversion equilibria for α-[Hasp-K] and six equilibria for β-[Hasp-K] complexes conformers were found and categorized as four single-step and one double-steps reactions for α-[Hasp-K] complex system, and four single-step and one double-steps for β-[Hasp-K] complex system as shown in Figs. S8 and S9. The most stable conformer of [Hasp-K] complex system is the conformer **3″** as shown in Fig. 3. The gas and aqueous phase relative B3LYP/6-311++G(d,p) energies, MIAs and DPEs for [Hasp-K] complex species are tabulated in Table 5. It shows that [Hasp-K] complex conformers are mostly in the single binding mode, except conformers **1″**–**3″**, **8″**, **9″** for α-[Hasp-K] complex type, conformers **17″**, **18″**, **21″** and **22″** for β-[Hasp-K] complex type. The relative stabilities are in decreasing order: **3″ > 22″ > 2″ ≈ 16″ > 9″ > 7″ > 14″ > 20″ > 21″ > 5″ > 4″ ≈ 6″ ≈ 12″ > 11″ > 18″ ≈ 13″ ≈ 1″ > 8″ > 15″ > 17″ > 19″ ≫ 10″.** Maximum values of both MIA and DPE are found in the conformer **2″**. The MIAs and DPEs of all [Hasp-K] complexes are within 105.14–124.91 kcal/mol and 320.41–351.81 kcal/mol, respectively. Interconversion reactions between 2 of 22 [Hasp-K] complexes with their transition states and their energies, thermodynamic properties, rate and equilibrium constants are shown in Table 6. As well as sodium complex, the aspartic ligand binds preferentially with potassium cation as tri-dentate mode. MIA difference between [Hasp_K] (118.05 kcal/mol) and $[asp\_K]^{-}$ (197.09 kcal/mol) is not very much when compare to sodium and lithium complexes.

3.4. Comparative reactions of aspartate complexes

Formation energies, Gibbs free energies of reaction, MIAs and pre-organization of aspartate conformers to form each complex are shown in Table 7. Relative stabilities of [Hasp-M] complexes are in order: [Hasp-Li] > [Hasp-Na] > [Hasp-K]. The BSSE energies for [Hasp-M] complexations are very small. Magnitudes of MIAs of [Hasp-M]–aspartate ligands are in order: [Hasp-Li]–aspartate > [Hasp-Na]–aspartate > [Hasp-K]–aspartate. The complexation reactions in gas phase are more preferable than in aqueous system by 155.47, 125.84 and 111.20 kcal/mol for lithium, sodium and potassium complexes, respectively. The pre-organization energies of [Hasp-M]–aspartate ligands are within a range of 10.20–17.01 kcal/mol

Table 3
Relative B3LYP/6-311++G(d,p) energies, MIAs and DPEs of minima for α-[Hasp-Na] and β-[Hasp-Na] complexes

Complexes/systems	Aspartate conformations	Binding mode	ΔE[a]	MIAs[a]	DPE[a]
α-[Hasp-Na]					
1′	γ_L [g$^-$ a][b]	α1	4.40	139.49	346.48
2′	γ_L [g$^-$ g$^-$][c]	α1	6.09	137.92	344.69
3′	γ_L [g$^+$g$^-$][d]	α1	2.53	131.17	348.26
4′	α_D [a g$^-$][e]	α1 + α4	8.41	135.78	342.37
5′	α_D [a g$^+$][f]	α1 + α4	1.88	142.21	348.91
6′	γ_D [a a][g]	α1 + α4	0.00	133.88	329.05
7′	α_L [g$^+$g$^-$][h]	α1	6.24	137.59	344.54
8′	γ_D [g$^+$g$^+$][i]	α1	4.12	121.58	346.66
9′	γ_D [a g$^-$][j]	α1 + α4	8.12	135.86	321.19
10′	γ_D [a g$^+$][k]	α1 + α4	2.36	142.02	326.95
11′	δ_D[g$^+$ g$^-$][l]	α5	10.72	133.41	318.33
12′	δ_D[g$^+$ a][m]	α5	3.76	140.69	325.29
β-[Hasp-Na]					
13′	ε_D[g$^-$g$^+$][b1]	β1	6.14	136.88	344.88
14′	γ_D[g$^-$ g$^+$][c1]	β1	6.72	137.47	344.31
15′	δ_D[g$^-$g$^+$][d1]	β1	4.33	130.68	346.69
16′	ε_D [a a][e1]	β1	7.87	134.98	343.16
17′	ε_D[a g$^-$][f1]	β1	2.53	123.17	348.50
18′	γ_D[g$^-$g$^+$][c1]	β1 + β2	9.72	134.58	331.85
19′	ε_D[g$^-$g$^+$][b1]	β1 + β2	7.87	135.26	333.70
20′	β_L[g$^+$g$^+$][g1]	β5	11.11	133.87	317.95
21′	δ_D[g$^+$g$^+$][h1]	β5	6.09	137.17	322.96
22′	δ_L[a g$^-$][i1]	β1 + β4	5.73	138.59	326.67
23′	β_L[a g$^-$][j1]	β1 + β4	1.41	133.66	330.99

[a]In kcal/mol with ZPE correction. [b]Identical to δ_L [g$^-$ g$^+$]. [c]Identical to δ_L [g$^-$ g$^+$]. [d]Identical to δ_L [g$^-$ a]. [e]Identical to γ_L [a g$^+$]. [f]Identical to α_L [a a]. [g]Identical to γ_L [a g$^-$]. [h]Identical to δ_D [g$^+$ g$^-$]. [i]Identical to γ_D [g$^+$ g$^+$]. [j]Identical to α_L [a g$^-$]. [k]Identical to δ_L [a g$^+$]. [l]Identical to β_L [g$^+$ g$^-$]. [m]Identical to β_L [g$^+$ a]. [b1]Identical to γ_D [g$^-$ g$^+$]. [c1]Identical to ε_D [g$^-$ g$^+$]. [d1]Identical to β_L [g$^-$ g$^+$]. [e1]Identical to γ_D [a a]. [f1]Identical to γ_D [a g$^-$]. [g1]Identical to β_L [g$^+$ g$^+$]. [h1]Identical to δ_D [g$^+$ g$^+$]. [i1]Identical to β_L [a g$^-$]. [j1]Identical to δ_D [a g$^-$].

Table 5
Relative B3LYP/6-311++G(d,p) energies, MIAs and DPEs of minima for α-[Hasp-K] and β-[Hasp-K] Complexes

Complexes/systems	Aspartate conformations	Binding mode	ΔE[a]	MIA[a]	DPE[a,b]
α-[Hasp-Na]					
1″	α_D [a g$^-$][b]	α1 + α4	8.69	119.77	346.49
2″	α_D [a g$^+$][c]	α1 + α4	3.37	124.91	351.81
3″	γ_D [a a][d]	α1 + α4	0.00	118.05	338.60
4″	γ_L [g$^-$ a][e]	α1	7.91	120.00	347.27
5″	γ_L [g$^-$ g$^-$][f]	α1	7.57	120.77	347.61
6″	α_L [g$^+$g$^-$][g]	α1	8.03	119.98	347.14
7″	γ_D [g$^+$g$^+$][h]	α1	4.57	105.14	350.43
8″	γ_D [a g$^-$][i]	α1 + α4	9.05	119.34	346.13
9″	γ_D [a g$^+$][j]	α1 + α4	3.94	124.28	351.24
10″	δ_D [g$^+$ g$^-$][k]	α5	14.97	113.26	320.41
11″	δ_D [g$^+$ a][l]	α5	8.38	120.14	326.99
β-[Hasp-K]					
12″	ε_D[g$^-$g$^+$][b1]	β1	8.08	119.11	347.09
13″	γ_D[g$^-$ g$^+$][c1]	β1	8.68	119.69	346.50
14″	δ_D[g$^-$g$^+$][d1]	β1	5.85	113.34	349.33
15″	ε_D[a a][e1]	β1	9.90	117.11	345.28
16″	ε_D[a g$^-$][f1]	β1	3.39	106.52	351.79
17″	ε_D[g$^-$g$^+$][b1]	β1 + β2	10.43	117.99	335.05
18″	γ_D[g$^-$g$^+$][c1]	β1 + β2	8.63	118.62	336.85
19″	δ_D[g$^+$g$^+$][g1]	β5	10.67	116.73	324.70
20″	β_L[g$^+$g$^+$][h1]	β5	6.85	121.70	328.52
21″	δ_L[a g$^-$][i1]	β1 + β4	7.29	121.17	331.31
22″	β_L[a g$^-$][j1]	β1 + β4	3.01	116.18	335.59

[a]In kcal/mol with ZPE correction. [b]Identical to γ_L [a g$^-$]. [c]Identical to γ_L [a g$^+$]. [d]Identical to α_L [a a]. [e]Identical to δ_L [g$^-$ g$^+$]. [f]Identical to δ_L [g$^-$ a]. [g]Identical to δ_D [g$^+$ g$^-$]. [h]Identical to γ_D [g$^+$ g$^+$]. [i]Identical to α_L [a g$^-$]. [j]Identical to δ_L [a g$^+$]. [k]Identical to β_L [g$^+$ g$^-$]. [l]Identical to β_L [g$^+$ a]. [b1]Identical to γ_D [g$^-$ g$^+$]. [c1]Identical to ε_D [g$^-$ g$^+$]. [d1]Identical to β_L [g$^-$ g$^+$]. [e1]Identical to γ_D [a a]. [f1]Identical to γ_D [a g$^-$]. [g1]Identical to β_L [g$^+$ g$^+$]. [h1]Identical to δ_D [g$^+$ g$^+$]. [i1]Identical to β_L [a g$^-$]. [j1]Identical to δ_D [a g$^-$].

(2.82–7.59 kcal/mol in aqueous system) and in order: [Hasp-Li] > [Hasp-Na] > [Hasp-K].

The energy gaps of free form aspartate conformers and their most stable complexes conformers are shown in Table 8. Based on the energy gaps, relative reactivities of seven conformers of [Hasp$^-$]-ligands are in decreasing order: $Hasp_{IV}{}^- > Hasp_V{}^- > Hasp_I{}^- > Hasp_{II}{}^- > Hasp_{VII}{}^- > Hasp_{VI}{}^- > Hasp_{III}{}^-$. Reactivities of [Hasp-M] complexes are in order: [Hasp-Li] > [Hasp-K] > [Hasp-Na].

Table 4
Thermodynamic quantities, equilibrium and rate constants of conversion reactions of the [Hasp-Na] complex systems, computed at B3LYP/6-311++G(d,p) level of theory

Reactions/systems[a]	$\Delta^{\ddagger}E$[b]	$\Delta^{\ddagger}G$[b]	ΔE_{298}[b]	ΔH_{298}[b]	ΔG_{298}[b]	K_{298}	k_{298}[c]
1′ → TSt1′_2′ → 2′	32.42	32.40	1.69	1.86	1.33	1.06×10^{-1}	1.11×10^{-11}
2′ → TSr2′_3′ → 3′	8.33	8.57	−3.56	−4.08	−2.72	9.82×10^{1}	3.22×10^{6}
4′ → TSt4′_5′ → 5′	26.50	27.05	−6.54	−6.71	−6.06	2.78×10^{4}	9.25×10^{-8}
5′ → TSr5′_6′ → 6′	9.09	9.64	−1.88	−2.22	−1.04	5.82×10^{0}	5.34×10^{5}
7′ → TSr7′8′ → 8′	8.02	8.84	−2.12	−2.29	−1.46	1.18×10^{1}	2.06×10^{6}
9′ → TSt9′_10′ → 10′	27.53	27.81	−5.76	−5.87	−5.45	9.96×10^{3}	2.53×10^{-8}
11′ → TSt11′12′ → 12′	26.97	27.01	−6.96	−6.99	−6.85	1.05×10^{5}	9.90×10^{-8}
13′ → TSt13′_14′ → 14′	32.30	32.25	0.57	0.58	0.36	5.42×10^{-1}	1.42×10^{-11}
14′ → TSr14′_15′ → 15′	10.83	10.90	−2.38	−2.60	−2.08	3.35×10^{1}	6.35×10^{4}
16′ → TSt16′_17′ → 17′	6.27	7.23	−5.34	−5.59	−4.38	1.62×10^{3}	3.11×10^{7}
18′ → TSt18′_19′ → 19′	31.85	31.91	−1.85	−1.85	−1.73	1.84×10^{1}	2.51×10^{-11}
20′ → TSt20′_21′ → 21′	33.93	34.40	5.01	4.47	6.15	3.10×10^{-5}	3.74×10^{-13}
22′ → TSr22′_23′ → 23′	11.93	11.60	−4.32	−4.47	−4.38	1.63×10^{3}	1.96×10^{4}

[a] The letters 'r' and 't' specify for the rotational (about C_β-CO_2 bond) transition-state and proton-transfer transition-state, respectively.
[b] In kcal/mol.
[c] In s^{-1}.

Table 6
Thermodynamic quantities, equilibrium and rate constants of conversion reactions of the [Hasp-K] complex systems, computed at B3LYP/6-311++G(d,p) level of theory

Reactions/systems[a]	$\Delta^{\ddagger}E$[b]	$\Delta^{\ddagger}G$[b]	ΔE_{298}[b]	ΔH_{298}[b]	ΔG_{298}[b]	K_{298}	k_{298}[c]
1″ → TSt1″_2″ → 2″	27.39	27.96	−5.32	−5.43	−4.80	3.28×10^{3}	1.98×10^{-8}
2″ → TSr2″_3″ → 3″	8.44	8.87	−3.37	−3.69	−2.74	1.01×10^{2}	1.95×10^{6}
4″ → TSt4″_5″ → 5″	30.75	30.61	0.34	0.48	0.01	9.82×10^{-1}	2.25×10^{-10}
6″ → TSr6″_7″ → 7″	8.01	8.36	−3.28	−3.46	−2.65	8.82×10^{1}	4.61×10^{6}
8″ → TSt8″_9″ → 9″	29.19	30.66	−5.11	−5.23	−4.50	1.99×10^{3}	2.07×10^{-10}
10″ → TSt10″_11″ → 11″	26.85	26.87	−6.59	−6.60	−6.53	6.17×10^{4}	1.25×10^{-7}
12″ → TSt12″_13″ → 13″	31.80	31.02	0.59	0.60	0.33	5.76×10^{-1}	1.13×10^{-10}
13″ → TSr13″_14″ → 14″	10.42	10.34	−2.82	−3.05	−2.50	6.80×10^{1}	1.63×10^{5}
15″ → TSr15″_16″ → 16″	4.28	6.30	−6.51	−6.80	−5.37	8.58×10^{3}	1.50×10^{8}
17″ → TSt17″_18″ → 18″	31.35	31.58	−1.80	−1.81	−1.62	1.55×10^{1}	4.43×10^{-11}
19″ → TSt19″_20″ → 20″	29.92	30.05	−3.82	−3.80	−3.74	5.49×10^{2}	5.81×10^{-10}
21″ → TSt21″_22″ → 22″	10.09	10.26	−4.28	−4.41	−4.81	3.34×10^{3}	1.87×10^{5}

[a] The letters 'r' and 't' specify for the rotational (about Cβ-CO_2 bond) transition-state and proton-transfer transition-state, respectively.
[b] In kcal/mol.
[c] In s^{-1}.

Table 7
Quantities for the formation reactions of the most stable conformers for [Hasp-M] complexes and pre-Organization for their aspartate structures, computed at the B3LYP/6-311++G(d,p) level of theory

Reaction	ΔE[a,b,c]	BSSE[a]	ΔE_{BSSE}[a]	MIA[a]	ΔG^{o}_{298}[a]
Complexation					
$[Hasp^{-}]_{\alpha_D\ [g^+\ a]} + Li^{+} \rightarrow [Hasp_{\delta_D\ [g^+\ a]}Li]_{\mathbf{19}}$	−168.53 (−13.06)	1.49	−167.03	169.76	−160.24
$[Hasp^{-}]_{\gamma_L[g^+g^-]} + Na^{+} \rightarrow [Hasp_{\gamma_D[a\ a]}Na]_{\mathbf{6'}}$	−133.34 (−7.50)	0.81	−132.53	133.88	−124.77
$[Hasp^{-}]_{\gamma_L\ [g^+\ g^-]} + K^{+} \rightarrow [Hasp_{\gamma_D\ [a\ a]}K]_{\mathbf{3'}}$	−117.68 (−6.48)	0.36	−117.32	118.05	−109.39
Pre-organization					
$[Hasp^{-}]_{\alpha_D\ [g^+\ a]} \rightarrow [Hasp^{-}]_{\delta_D\ [g^+\ a]_{\mathbf{19}}}$	17.01 (7.59)	–	–	15.74[d]	19.07
$[Hasp^{-}]_{\gamma_L\ [g^+\ g^-]} \rightarrow [Hasp^{-}]_{\gamma_D\ [a\ a]_{\mathbf{6'}}}$	13.67 (5.18)	–	–	13.71[d]	14.12
$[Hasp^{-}]_{\gamma_L\ [g^+\ g^-]} \rightarrow [Hasp^{-}]_{\gamma_D\ [a\ a]_{\mathbf{3''}}}$	10.20 (2.82)	–	–	10.22[d]	10.58

[a] In kcal/mol.
[b] The ZPVE corrected energies.
[c] In vacuo and aqueous using CPCM solvent effect (in parenthesis), in kcal/mol.
[d] Enthalpy in kcal/mol.

3.5. Binding mode and ion size effects

The most stable [Hasp-M] complexes were found as tri-coordinated form (α5 mode) for the lithium complex and as bi-coordinated form (α1 + α4 combine mode) for the complexes of sodium and potassium as shown Fig. 3. Table 9 shows that the average bond-distances of M^{+}–O bond for the [Hasp-M] complexes are in order: [Hasp-K]-bond > [Hasp-Na]-bond > [Hasp-Li]-bond which corresponds to the order of ionic size: potassium (r_K = 1.548 Å) > sodium (r_{Na} = 1.1 Å) and lithium (r_{Li} = 0.76 Å). The ion sizes of potassium and sodium ions obviously affect the coordination of the complexes with $Hasp^{-}$ (see Fig. 3). This ionic size effect has never occurred in their complexes with aspartate dianion (asp^{2-} species) [41].

3.6. Reaction paths to form [Hasp_M] complexes

As complexation based on the asp^{2-} species is considered, the [Hasp-M] complexes, M = Li^{+}, Na^{+} and K^{+} can be formed via protonation and complexation processes using two reaction pathways as shown in Fig. 4. It shows that top and bottom paths

Table 8
The frontier molecular orbital energy gap, $\Delta E_{HOME–LIMO}$ free form aspartate and the most stable complex conformers for [Hasp-M] computed at the B3LYP/6-311++G(d,p) level

Species	$\Delta E_{HOME–LIMO}$[a]
$Hasp_{\mathbf{I}}^{-}$[b]	4.41
$Hasp_{\mathbf{II}}^{-}$[c]	4.30
$Hasp_{\mathbf{III}}^{-}$[d]	3.86
$Hasp_{\mathbf{IV}}^{-}$[e]	5.44
$Hasp_{\mathbf{V}}^{-}$[f]	4.57
$Hasp_{\mathbf{VI}}^{-}$[g]	4.03
$Hasp_{\mathbf{VII}}^{-}$[h]	4.14
$[Hasp\text{-}Li]_{\mathbf{19}}$	4.79
$[Hasp\text{-}Na]_{\mathbf{6'}}$	5.74
$[Hasp\text{-}K]_{\mathbf{3''}}$	5.61

[a] In eV.
[b] Belongs to γ_L [g^+ g^-] conformation.
[c] Belongs to γ_L [g^+ g^+] conformation.
[d] Belongs to α_D [g^+ a] conformation.
[e] Belongs to γ_L [a g^-] conformation.
[f] Belongs to δ_D [g^- g^+] conformation.
[g] Belongs to α_D [g^+ g^+] conformation.
[h] Belongs to γ_D [g^+ g^+] conformation.

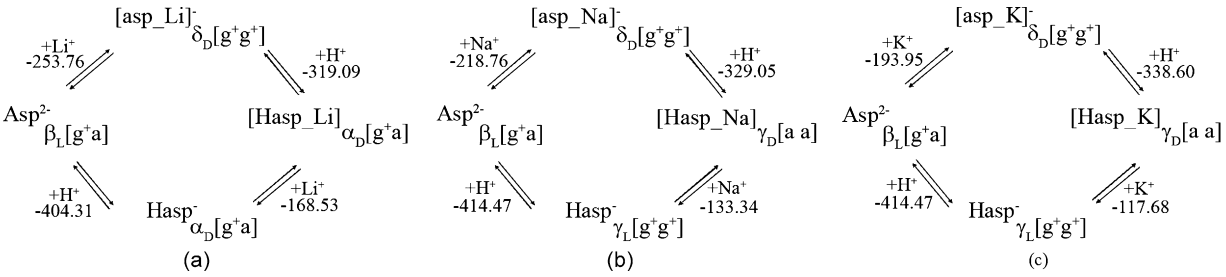

Fig. 4. The reaction pathways for complexation and protonation of asp^{2-} species to form [Hasp-M] complexes of (a) lithium, (b) sodium and (c) potassium. Energies are in kcal/mol.

Table 9
Bond distances of alkali metal cations and binding atoms of aspartate ions in the most stable conformers of [Hasp-M] complexes, computed at the B3LYP/6-311++G(d,p) level

Bonds/distances[a]	Complexes		
	[Hasp-Li][b]	[Hasp-Na][c]	[Hasp-K][c]
M^+–N	2.060	–	–
M^+–O_1	1.815	2.357	2.670
M^+–O_2	–	2.275	2.614
M^+–O_4	1.945	2.354	2.734

[a] In Å.
[b] Defined as α5 binding mode.
[c] Defined as α1 + α4 binding mode.

belong to reaction sequences of complexation → protonation and protonation → complexation, respectively. The protonation of asp^{2-} species to form $Hasp^-$ species being more likely to occur than the complexation of $[asp\_M]^-$ to form [Hasp_M] complex. Therefore, protonation → complexation sequence is predicted to be the most preferable pathway of the [Hasp-M] complex formation. The energies of overall reactions to form complexes with lithium, sodium and potassium are −572.82, −547.81 and −532.55 kcal/mol, respectively. The conformers of asp^{2-}, $Hasp^-$, $[asp\_M]^-$ and [Hasp_M] shown in Fig. 4 are significant because they correspond to their structural reaction coordinates.

4. Conclusions

The B3LYP/6-311++G(d,p)-optimized structures of all conformers of α- and β-[Hasp-M] complexes were obtained. Numbers of 39 conformers for [Hasp-Li], 23 conformers for [Hasp-Na] and 22 conformers for [Hasp-K] complexes were found. Based on their single-step interconversions, numbers of 28 equilibria for [Hasp-Li], 13 equilibria for [Hasp-Na] and 12 equilibria for [Hasp-Li] complex systems were found and their corresponding transition-state structures were obtained. The most stable conformers of [Hasp-M] complexes are α-[Hasp-Li]$_{\mathbf{19}}$, α-[Hasp-Na]$_{\mathbf{6'}}$ and α-[Hasp-K]$_{\mathbf{3''}}$ of which binding energies are −168.53, −133.34 and −117.68 kcal/mol, respectively. Relative stabilities and reactivities of [Hasp-M] complexes are in orders: [Hasp-Li] > [Hasp-Na] > [Hasp-K] and [Hasp-Li] > [Hasp-K] > [Hasp-Na], respectively. Magnitudes of MIAs of [Hasp-M]–aspartate ligands are in order: [Hasp-Li]–aspartate > [Hasp-Na]–aspartate > [Hasp-K]–aspartate. Relative reactivities of seven conformers of $[Hasp^-]$-ligands are in decreasing order: $Hasp_{IV}^- > Hasp_V^- > Hasp_I^- > Hasp_{II}^- > Hasp_{VII}^- > Hasp_{VI}^- > Hasp_{III}^-$. The average bond-distances of M^+–O bonds of the [Hasp-M] complexes are in order: [Hasp-K]-bond > [Hasp-Na]-bond > [Hasp-Li]-bond. The most stable complex conformer as a tri-coordinated form for aspartate complex with Li^+ and bi-coordinated form for aspartate complexes with Na^+ and K^+ were found.

Acknowledgements

This work was financially supported by the Thailand Research Fund (TRF). The Royal Golden Jubilee (RGJ) grant, number PHD46K0087 supported by TRF to WS was acknowledged.

Appendix A. Supplementary data

Supplementary data associated with this article can be found, in the online version, at doi:10.1016/j.jmgm.2007.08.004.

References

[1] J.H. Jensen, M.S. Gordon, On the number of water molecules necessary to stabilize the glycine zwitterion, J. Am. Chem. Soc. 117 (1995) 8159–8170.
[2] J.P. Gluster, Structural aspects of metal liganding to functional groups in proteins, Adv. Protein Chem. 42 (1991) 1–76.
[3] S.A. Lippard, J.M. Berg, Principles of Bioinorganic Chemistry, University Science Books, Mill Valley, CA, 1994.
[4] M.N. Hughes, The Inorganic Chemistry of Biological Process, 2nd ed., John Wiley and Sons, Chichester, 1981.
[5] D.A. Dougherty, Cation interactions in chemistry and biology: a new view of benzene, Phe, Tyr, and Trp, Science 271 (1996) 163–168.
[6] B.S. Freiser (Ed.), Organometallic Ion Chemistry, Kluwer, Dordrecht, 1996.
[7] W. Kaim, B. Schwederski, Bioinorganic Chemistry: Inorganic Elements in Chemistry of Life, Wiely, Chichester, 1994.
[8] R.A. Jockusch, W.D. Price, E.R. Williams, Structure of cationized arginine (Arg_M^+, M = H, Li, Na, K, Rb, and Cs) in the gas phase: further evidence for zwitterionic arginine, J. Phys. Chem. A 103 (1999) 9266–9274.
[9] E.F. Strittmatter, A.S. Lemoff, E.R. Williams, Structure of cationized glycine, Gly_M^{2+} (M = Be, Mg, Ca, Sr, Ba), in the gas phase: intrinsic effect of cation size on zwitterion stability, J. Phys. Chem. A 104 (2000) 9793–9796.
[10] T. Marino, N. Russo, M. Toscano, Gas-phase metal ion (Li^+, Na^+, Cu^+) affinities of glycine and alanine, J. Inorg. Biochem. 79 (2000) 179–185.
[11] T. Marino, N. Russo, M. Toscano, Potential energy surfaces for the gas-phase interaction between α-alanine and alkali metal ions (Li^+, Na^+, K^+). A density functional study, Inorg. Chem. 40 (2001) 6439–6443.

[12] T. Marino, N. Russo, M. Toscano, Interaction of Li^+, Na^+, and K^+ with the proline amino acid. Complexation modes, potential energy profiles, and metal ion affinities, J. Phys. Chem. B 107 (2003) 2588–2594.
[13] S. Pulkkinen, M. Noguera, L. Rodríguez-Santiago, M. Sodupe, J. Bertran, Gas phase intramolecular proton transfer in cationized glycine and chlorine substituted derivatives (M-Gly, M = Na^+, Mg^{2+}, Cu^+, Ni^+, and Cu^{2+}): Existence of zwitterionic structures? Chem.-Eur. J. 6 (2000) 4393–4399.
[14] M. Remko, B.M. Rode, Effect of metal ions (Li^+, Na^+, K^+, Mg^{2+}, Ca^{2+}, Ni^{2+}, Cu^{2+}, and Zn^{2+}) and water coordination on the structure of glycine and zwitterionic glycine, J. Phys. Chem. A 110 (2006) 1960–1967.
[15] B.M. Yu, P. Paroutis, A.R. Davidson, P.L. Howell, Disruption of a salt bridge dramatically accelerates subunit exchange in duck delta2 crystallin, J. Biol. Chem. 279 (2004) 40972–40979.
[16] A.M. de Vos, M. Ulsch, A.A. Kossiakoff, Human growth hormone and extracellular domain of its receptor: crystal structure of the complex, Science 255 (1992) 306–312.
[17] S.W. Lee, H.S. Kim, J.L. Beauchamp, Salt bridge chemistry applied to gas-phase peptide sequencing: selective fragmentation of sodiated gas-phase peptide ions adjacent to aspartic acid residues, J. Am. Chem. Soc. 120 (1998) 3188–3195.
[18] L.M. Teesch, R.C. Orlando, J. Adams, Location of the alkali metal ion in gas-phase peptide complexes, J. Am. Chem. Soc. 113 (1991) 3668.
[19] X.J. Tang, P. Thibault, R.K. Boyd, Structure of cationized arginine (Arg_M^+,M = H, Li, Na, K, Rb, and Cs) in the gas phase: further evidence for zwitterionic arginine, Org. Mass Spectrom. 28 (1993) 1047–1050.
[20] R.C. Dunbar, Complexation of Na^+ and K^+ to aromatic amino acids: a density functional computational study of cation–π interactions, J. Phys. Chem. A 104 (2000) 8067–8074.
[21] C. Ruan, M.T. Rodgers, Cation–π interactions: structures and energetics of complexation of Na^+ and K^+ with the aromatic amino acids, phenylalanine, tyrosine, and tryptophan, J. Am. Chem. Soc. 126 (2004) 14600–14610.
[22] T. Wyttenbach, M. Witt, M.T. Bowers, On the question of salt bridges of cationized amino acids in the gas phase: glycine and arginine, Int. J. Mass Spectrom. 183 (1999) 243–252.
[23] T. Wyttenbach, M. Witt, M.T. Bowers, On the stability of amino acid zwitterions in the gas phase: the influence of derivatization, proton affinity, and alkali ion addition, J. Am. Chem. Soc. 122 (2000) 3458–3464.
[24] R.A. Jockusch, A.S. Lemoff, E.R. Williams, Effect of metal ion and water coordination on the structure of a gas-phase amino acid, J. Am. Chem. Soc. 123 (2001) 12255–12265.
[25] R.A. Jockusch, A.S. Lemoff, E.R. Williams, Hydration of valine-cation complexes in the gas phase: on the number of water molecules necessary to form a zwitterion, J. Phys. Chem. A 105 (2001) 10929–10942.
[26] A.S. Lemoff, E.R. Williams, Binding energies of water to lithiated valine: formation of solution-phase structure in vacuo, J. Am. Soc. Mass Spectrom. 15 (2004) 1014–1024.
[27] A.S. Lemoff, M.F. Bush, E.R. Williams, Binding energies of water to sodiated valine and structural isomers in the gas phase: the effect of proton affinity on zwitterion stability, J. Am. Chem. Soc. 125 (2003) 13576–13584.
[28] A.S. Lemoff, M.F. Bush, E.R. Williams, Structures of cationized proline analogues: evidence for the zwitterionic form, J. Phys. Chem. A 109 (2005) 1903–1910.
[29] A.S. Lemoff, M.F. Bush, C.C. Wu, E.R. Williams, Structures and hydration enthalpies of cationized glutamine and structural analogues in the gas phase, J. Am. Chem. Soc. 127 (2005) 10276–10286.
[30] M.M. Kish, G. Ohanessian, C. Wesdemiotis, The relative Na^+ affinities of α-amino acids: side-chain substituent effects, Int. J. Mass Spectrom. 227 (2003) 509–524.
[31] H.A. Cox, R.R. Julian, S.W. Lee, J.L. Beauchamp, Gas-phase H/D exchange of sodiated glycine oligomers with ND3: exchange kinetics do not reflect parent ion structures, J. Am. Chem. Soc. 126 (2004) 6485–6490.
[32] M. Rožman, B. Bertoša, L. Klasinc, D. Srzić, Gas phase H/D exchange of sodiated amino acids: why do we see zwitterions? J. Am. Soc. Mass Spectrom. 17 (2006) 29–36.
[33] S.J. Ye, R.M. Moision, P.B. Armentrout, Sequential bond energies of water to sodium glycine cation, Int. J. Mass Spectrum. 240 (2005) 233–248.
[34] M.T. Rodgers, P.B. Armentrout, A thermodynamic "vocabulary" for metal ion interactions in biological systems, Acc. Chem. Res. 37 (2004) 989–998.
[35] R.M. Moision, P.B. Armentrout, Experimental and theoretical dissection of sodium cation/glycine interactions, J. Phys. Chem. A 106 (2002) 10350–10362.
[36] R.M. Moision, P.B. Armentrout, An experimental and theoretical dissection of potassium cation/glycine interactions, Phys. Chem. Chem. Phys. 6 (2004) 2588–2599.
[37] N.C. Polfer, B. Paizs, L.C. Snoek, I. Compagnon, S. Suhai, G. Meijer, G. von Helden, J. Oomens, Infrared fingerprint spectroscopy and theoretical studies of potassium ion tagged amino acids and peptides in the gas phase, J. Am. Chem. Soc. 127 (2005) 8571–8579.
[38] W. Sang-aroon, V. Ruangpornvisuti, Conformational study of cationic, zwitterionic, anionic species of aspartic acid, water-added forms and their protonation. A DFT method, J. Mol. Struct. (THEOCHEM) 758 (2006) 181–187.
[39] W.Y. Feng, S. Gronert, C. Lebrilla, The lithium cation binding energies of gaseous amino acids, J. Phys. Chem. A 107 (2003) 405–410.
[40] A. Gapeev, R.C. Dunbar, Na^+ affinities of gas phase amino acids by ligand exchange equilibrium, Int. J. Mass Spectrom. 228 (2003) 825–839.
[41] W. Sang-Aroon, V. Ruangpornvisuti, Conformational analysis of alkali metal complexes of aspartate dianion and their interactions in gas phase, J. Mol. Graph. Model. 26 (2007) 342–351.
[42] A.D. Becke, Density-functional thermochemistry. III. The role of exact exchange, J. Chem. Phys. 98 (1993) 5648–5652.
[43] C. Lee, W. Yang, R.G. Parr, Development of the Colle–Salvetti correlation-energy formula into a functional of the electron density, Phys. Rev. B 37 (1988) 785–789.
[44] V. Barone, M. Cossi, J. Phys. Chem A 102 (1998) 1995–2001.
[45] M.J. Frisch, J.E. Del Bene, J.S. Binkley, H.F. Schhaefer III, Extensive theoretical studies of the hydrogen-bonded complexes $(H_2O)_2$, $(H_2O)_2H^+$, $(HF)_2$, $(HF)_2H^+$, F_2H^-, and $(NH_3)_2$, J. Chem. Phys. 84 (1986) 2279–2289.
[46] D.W. Schwenke, D.G. Truhlar, Systematic study of basis set superposition errors in the calculated interaction energy of two HF molecules, J. Chem. Phys. 82 (1985) 2418–2426.
[47] M.J. Frisch, G.W. Trucks, H.B. Schlegel, G.E. Scuseria, M.A. Robb, J.R. Cheeseman, J.A. Montgomery Jr., T. Vreven, K.N. Kudin, J.C. Burant, J.M. Millam, S.S. Iyengar, J. Tomasi, V. Barone, B. Mennucci, M. Cossi, G. Scalmani, N. Rega, G.A. Petersson, H. Nakatsuji, M. Hada, M. Ehara, K. Toyota, R. Fukuda, J. Hasegawa, M. Ishida, T. Nakajima, Y. Honda, O. Kitao, H. Nakai, M. Klene, X. Li, J.E. Knox, H.P. Hratchian, J.B. Cross, C. Adamo, J. Jaramillo, R. Gomperts, R.E. Stratmann, O. Yazyev, A.J. Austin, R. Cammi, C. Pomelli, J.W. Ochterski, P.Y. Ayala, K. Morokuma, G.A. Voth, P. Salvador, J.J. Dannenberg, V.G. Zakrzewski, S. Dapprich, A.D. Daniels, M.C. Strain, O. Farkas, D.K. Malick, A.D. Rabuck, K. Raghavachari, J.B. Foresman, J.V. Ortiz, Q. Cui, A.G. Baboul, S. Clifford, J. Cioslowski, B.B. Stefanov, G. Liu, A. Liashenko, P. Piskorz, I. Komaromi, R.L. Martin, D.J. Fox, T. Keith, M.A. Al-Laham, C.Y. Peng, A. Nanayakkara, M. Challacombe, P.M.W. Gill, B. Johnson, W. Chen, M.W. Wong, C. Gonzalez, J.A. Pople, Gaussian 03, Revision D. 02, Gaussian, Inc., Pittsburgh, PA, 2006.
[48] G. Schaftenaar, Molden 3.7, CAOS/CAMM Center, Nijmegen Toernooiveld, Nijmegen, Netherlands, 1991.
[49] P. Flükiger, H.P. Lüthi, S. Portmann, J. Weber, Molekel 4.3, Swiss Center for Scientific Computing, Manno, Switzerland, 2000.